

# International Conference on Space Optics—ICSO 2022

Dubrovnik, Croatia

3–7 October 2022

*Edited by Kyriaki Minoglou, Nikos Karafolas, and Bruno Cugny,*



## *Extending Atmospheric Propagation Time Series of Satellites Optical Feeder-Links: a System Analysis Approach*



---

# Extending Atmospheric Propagation Time Series of Satellites Optical Feeder-Links: a System Analysis Approach

Tarik Benaddi<sup>a</sup> and Lucien Canuet<sup>\*b</sup>

<sup>a</sup>Thales Alenia Space, Toulouse, France

<sup>b</sup>ESA/ESTEC, Noordwijk, Netherlands

## ABSTRACT

Atmospheric propagation channels of satellite-to-ground optical links are hard to model and are rather represented with time series generated using complex emulators. In this paper, we propose a simple framework which, from an arbitrary time series, generates rapidly similar series that exhibit the same system-level performance. The goal of such generated time series is not to model differently the channel but rather to assist in analysing the system performance (synchronization, error correction code, interleaving . . .) and also in evaluating equipment behavior for free-space laser propagation through atmospheric turbulence.

## 1. INTRODUCTION

The adoption of satellites as a communication medium for multimedia connectivity systems requires optimization of the cost per bit transmitted in order to remain competitive with terrestrial solutions. For systems dedicated to broadband connectivity, increasing the total capacity of the system is a natural solution to achieve this objective. In this context, Free Space Optical (FSO) Communications on feeder links is a promising solution for the future generation of Very High Throughput Satellites<sup>1-3</sup> in geosynchronous orbit (GEO). Besides increasing the capacity, FSO payloads may offer many advantages in comparison to their RF counterparts like (reduced number of gateways, spectrum availability and regulation, lower size and weight of the satellite's feeder section. . .). However, these come at the expense of new challenges such as the fact that optical links through the atmosphere are subject to more adverse propagation effects. These later are notably due to the propagation channel (clouds, aerosols, optical atmospheric turbulence. . . that are site location-dependant) on one hand and due to the optical front-end design (from the optical head to the specific photonic sub-systems) on the other. Obtaining accurate analytical and developing end-to-end simulators or models relevant to satellite-to-ground optical propagation channel alone is very challenging even if some approximations were proposed in the literature (cf<sup>4</sup> and therein references).

To the authors knowledge, the most reliable models that are used currently to assess optical feeder link design and analysis are rather based on times series (TS). TS represents the varying received optical power during time and can be obtained either via real ground-onboard transmissions using a simplified architecture<sup>5,6</sup> or via proprietary optical channel simulators configured with the right physical parameters.<sup>4,7</sup> Relevant and representative experiments are not widely spread as GEO feeder telecommunications through the atmosphere are still at early stages. Accurate simulated data able to cover a wide range of relevant propagation parameters are costly to generate as they often rely on complex wave-optics coupled to end-to-end mitigation systems simulators. They often require a non-negligible amount of simulation time (depending on the configuration) in order to obtain a-few-seconds-long time series.

In this paper, we address the case where we have a relevant but short TS representation of a given ground-to-GEO transmission scenario. Often, system engineers aiming at conducting end-to-end performance analyses and optimizations require longer series with different statistical realizations. This enables Monte Carlo system analyses used for the reliable prediction of fading and inter-fading durations used to evaluate error correction code performance, modem synchronization thresholds and re-synchronization delays, channel interleaver design and their impact on service availability. We propose a framework that allows to generate, from a given TS (either acquired using actual transmissions or generated with advanced optical channel simulators), new TS series of

---

\* This study was conducted when Lucien Canuet was still employed at Thales Alenia Space.

any length on the fly. Our goal is not to generate TS that represent more reliably the aforementioned optical transmission effects, but rather that assist analysing the system performance (synchronization, error correction code, interleaving . . .) and evaluating equipment behavior for free-space laser propagation through atmospheric turbulence. To this aim, we propose a two-fold framework: first using a distribution fitting procedure to approach the statistical gain of the atmospheric optical channel and second using a discrete Markov state machine to model the time correlation of the TS.

This paper is organized as follows. We introduce our system architecture and the underlying TS. Then, our proposed framework to model and generate such time series is described. And finally, the obtained results are presented and discussed.

## 2. SYSTEM DESCRIPTION

The optical feeder link considered in this paper implements a half optical link from the optical ground station (OGS) to the satellite followed by a half radio-frequency (RF) link from the satellite to the end users. This architecture is depicted in Fig. 1.

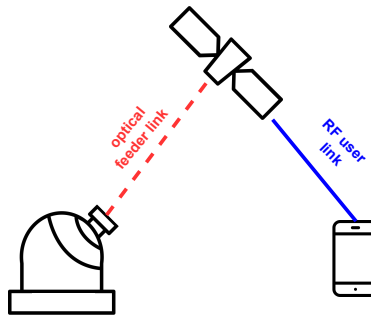


Figure 1: Considered optical feeder link scenario

The end-to-end performance of the physical layer in this case is complex to simulate in comparison to a conventional RF transmission. In particular, it is essential to know the impact of the optical half-link on the overall performance in order to reliably dimension the optical link. Optical links through the atmosphere are subject to different propagation effects than RF links. The optical spectrum that is envisioned is located primarily in the C-band [1530-1565 nm] and in the L-band [1565-1625 nm]. At such wavelengths, the optical propagation phenomena in the atmosphere can be divided into two main classes:

- Macro-scale phenomena: (i) blocking caused by most water clouds, (ii) absorption caused by molecules and (iii) scattering caused by aerosols.
- Micro-scale phenomena: non-symmetrical propagation effects between the uplink and the downlink induced by optical turbulence and that can vary on relatively small geographical and time scales.

These impairments can be very complicated to model analytically because (i) macro-scale phenomena depends on various physical and chemical parameters and (ii) optical turbulence theory coupled to mitigation techniques such as adaptive optics can rarely be captured by simple analytical frameworks. Consequently and in order to assess the impact of the propagation channel during design phase, we generally resort to simulated TS to evaluate the optical communication system (OCS) performance. Such TS can represent, for instance, the coupled optical flux in a single mode component characterizing the input of receiving OCS. The stochastic nature of such variations depends on various parameters such as the characteristic turbulence and wind profiles, adaptive optics (AO) correction, telescope diameter and link elevation. Figure 2 plots an example of a downlink coupled optical flux for a given set of system parameters. \*

\*This TS has been generated by ONERA under CNES contract using the turbulence simulation tools Turandot and the AO simulation tool (AOST) which generate both uplink and downlink AO compensated time series<sup>4</sup>

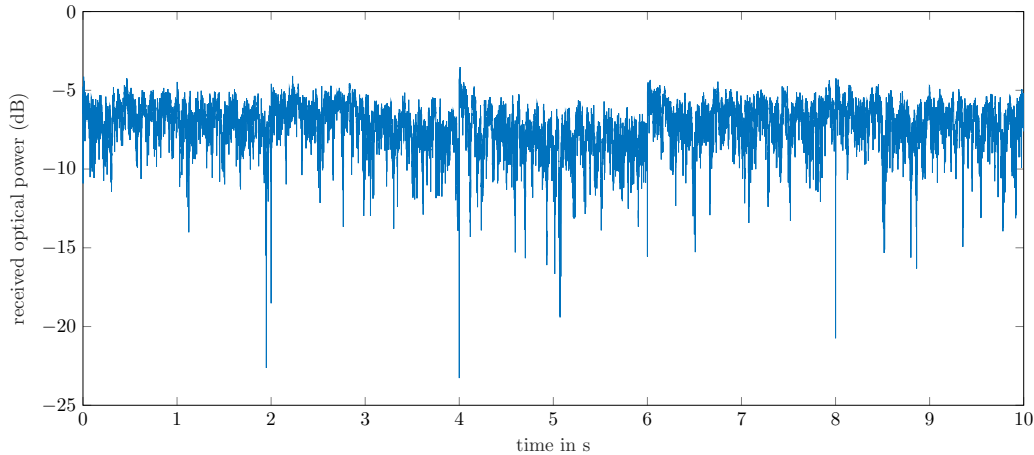


Figure 2: An example of a TS representing the optical flux received at the optical ground station from a GEO satellite

In order to evaluate the performance of an end-to-end transmission scheme, one would like to have sufficiently long (and thus statistically representative) time series. This makes the use of these TS generators on the fly not convenient since they must run during a long time in order to generate a few-seconds-long TS.

A framework which allows to generate, from a parent TS and on the fly, similar TS of independent realizations is detailed in the following section.

### 3. PROPOSED FRAMEWORK

As mentioned above, our goal is not to reproduce a time series as finely as possible, but rather to generate time series with different statistical realizations than the original one. To this aim, we mainly focus on the attenuation variations which directly impact the levels of the signal-to-noise ratio at the reception and the digital signal processing algorithms performance (clock and carrier synchronization threshold, forward-error correction (FEC) decoding performance...). The impact of these correlated attenuation can be reduced to two main characteristics:

- Their distribution: i.e. the probability with which one can observe the different realizations of these attenuation. This distribution impacts the decoding threshold of the physical layer algorithms. We are therefore naturally interested here in their probability density function (PDF).
- Their evolution in time: i.e. the probability to observe a given future attenuation knowing the previous measurements. This temporal correlation plays an important role in the behavior of the physical layer algorithms that exhibits memory (filters, interleavers, feedback loops ...)<sup>8</sup>

Consequently, in order to generate a new TS from a parent TS, we implement the following two steps:

- Generate a TS that matches, from a statistical point of view, the distribution of the parent TS.
- Introduce a temporal correlation by judiciously rearranging the previously obtained realizations.

#### 3.1 Distribution fitting

Optical power attenuation induced by optical atmospheric turbulence are widely modeled using various distributions such as the log-normal, the exponential or the gamma-gamma distribution.<sup>9–11</sup>

Without loss of generality, we focus hereafter on the TS illustrated in Fig. 2. The corresponding PDF is shown in Fig. 3a and was found to be very well fit using a log-normal PDF with mean  $\mu = 1.255$  and variance  $\sigma = 0.399$ . Also, to estimate the quality of service of the system in terms of availability, we may also consider the cumulative density function (CDF). The original CDF and the obtained one are also plotted in Fig. 3b.

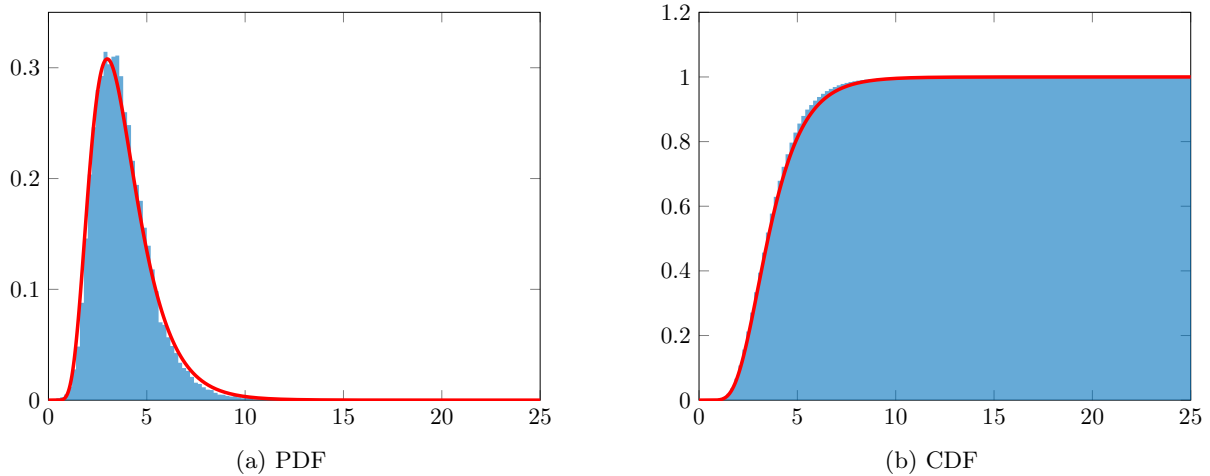


Figure 3: PDF and CDF of the parent TS (blue histogram) and the corresponding log-normal distribution fitting (red line). The values of the TS points were converted to corresponding positive values for a natural distribution fitting

It is worth noting that this distribution fitting can be further improved considering other more specific distributions or mixture of distributions (as for instance<sup>12</sup>). However, in this case, log-normal distribution was found to present satisfying end-to-end performance analysis results.

### 3.2 Time correlation

The TS depicted in Fig. 2 presents samples that are correlated in time. This phenomenon is of high interest for the system analysis as it defines the fading and inter-fading statistics. The fading, defined as the received power threshold below which the receiver is not able to retrieve data, can last from a fraction of millisecond to longer than 10ms for GEO-to-ground scenarios. Consequently, repeated and long fading will cause frequent transmission interruptions.

To model this behavior, we consider discrete Markov chains. A discrete Markov chain is a stochastic process that consists of a finite number of states and transition probabilities to go from one state to the other. In this paper, we consider only first-order Markov chain processes in which the conditional probability for getting to a given state depends only on the current state of the system. One of the most simple and well studied Markov chain models in digital communications is the Gilbert-Elliot (GE) model.<sup>13</sup> It is a time varying channel defined by two states: each state is defined by a binary symmetric channel (BSC) with a given crossover probability. The two states are commonly designated  $\mathcal{G}$  for a good channel (i.e. low crossover probability) and  $\mathcal{B}$  for a bad channel (i.e. a higher crossover probability).

Unlike the GE model which is on the bit level, we would like to have a Markov chain (MC) on the analog signal domain and having more than 2 states: each state is defined by fading within a given range of amplitudes. Let us suppose that our TS presents receiver optical powers (or equivalently channel attenuation) ranging between a maximum value  $\mathcal{T}_{max}$  and an minimum value  $\mathcal{T}_{min}$ . Let us define the MC states following a partition of the interval  $[\mathcal{T}_{min}, \mathcal{T}_{max}]$  whose boundaries are given by the real sequence  $\mathcal{T}_{min} = \mathcal{T}_0 \leq \mathcal{T}_1 \leq \dots \leq \mathcal{T}_i \leq \dots \leq \mathcal{T}_n = \mathcal{T}_{max}$ . In other terms, the state  $\sigma_i$  is defined as the set of amplitudes laying within the interval  $]\mathcal{T}_i, \mathcal{T}_{i+1}]$ .

Therefore, as for the GE channel and depending on the state in which our TS generator is, it will output a random received powers comprised between the boundaries of the interval that defines the current state. In this paper, we consider only uniformly distributed sampling. Thus, during calibration phase using the parent TS, it is worth mentioning that there are two main features to optimize in this MC-based generator: the boundaries spacing  $\{\mathcal{T}_i\}_i$  and the total number of states  $n$ .

The boundaries  $\{\mathcal{T}_i\}_i$  can be chosen to be distributed linearly, logarithmically or following any other spacing strategy. Figure 4 illustrates the linear spacing strategy where the boundaries are equidistributed in the interval

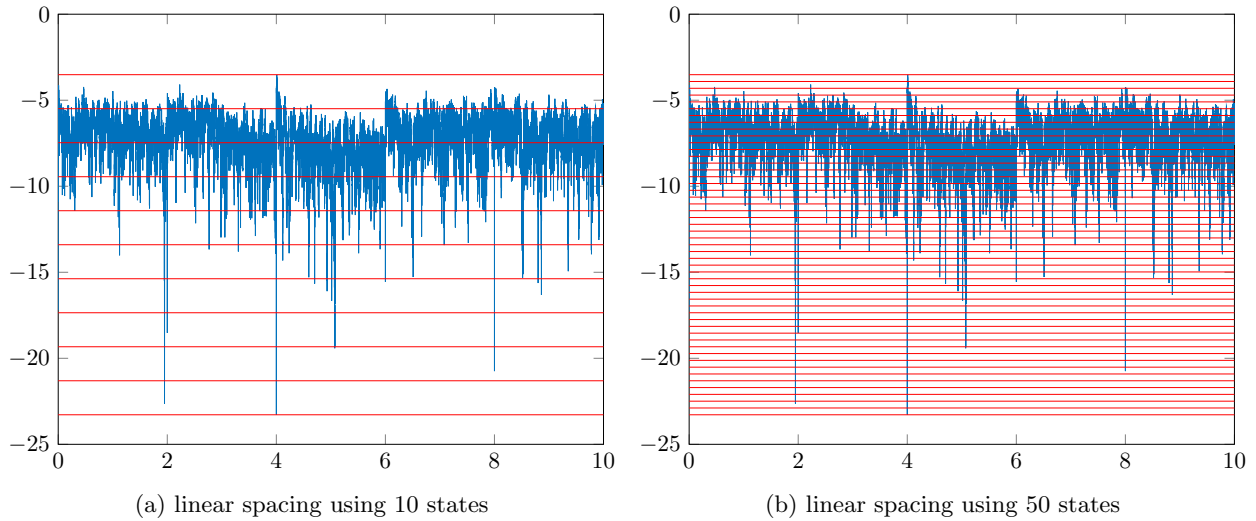


Figure 4: Linear spacing strategy showing the boundaries values  $\{\mathcal{T}_i\}_i$

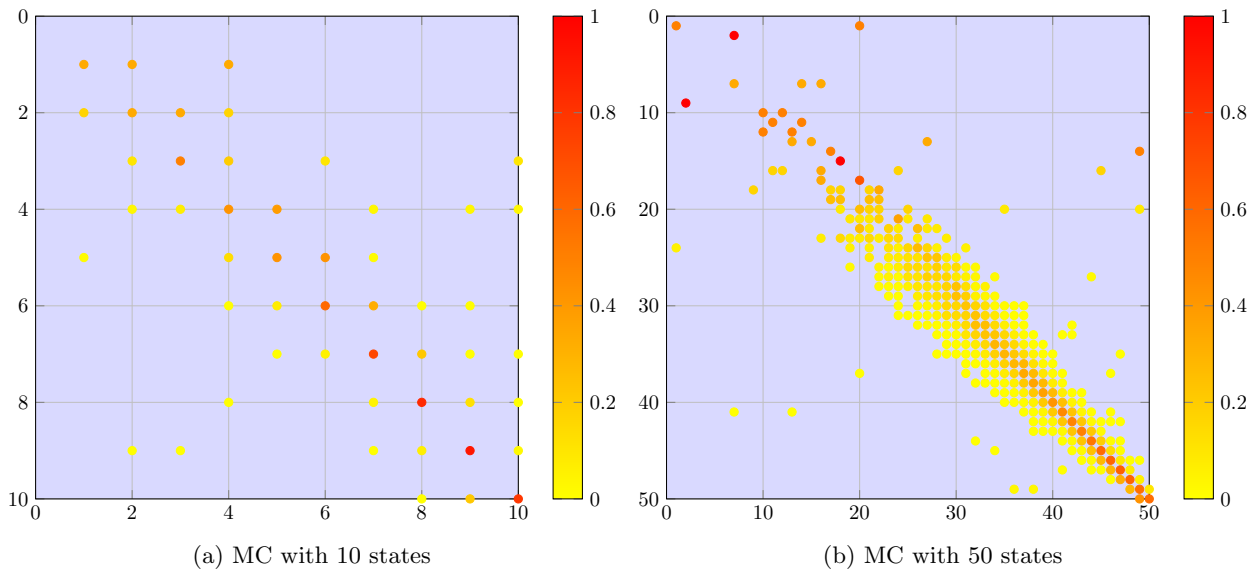


Figure 5: Transition matrix learnt from the parent TS

$[\mathcal{T}_{min}, \mathcal{T}_{max}]$ . The amplitudes in the bottom-most interval, here  $[-23.28, -21.30]$  in Fig. 4a is defined as the worst channel state or  $\sigma_0$ .

Regarding the transition matrix, if the number of states is too low, for instance 2 as in the GE model, the generated TS will exhibit few bins (2 for GE) in which the amplitudes are going to be generated uniformly. If the number of states is too high, the probabilities in the transition matrix will be too close to each other, at least in the high amplitudes region, and the original TS may be not sufficiently long to allow a good estimation of the transition matrix. Figures 5a and 5b illustrates the transition matrices corresponding to the TS and the state partitions described in Fig. 4.

We observe that due to the time correlation of the TS, the highest probabilities occur on the diagonal of the matrix. This means that, if the current channel state is known, it is most probable that the next attenuation will be within the same or an adjacent amplitude range. Moreover, the matrix become sparse in the bad channel states region (the up region of the transition matrix), which means that once we visit a bad state, we tend to jump to a better state with high probability. A behavior that is explained by the fact that the deep fading regions are steep and sparse in the time domain.

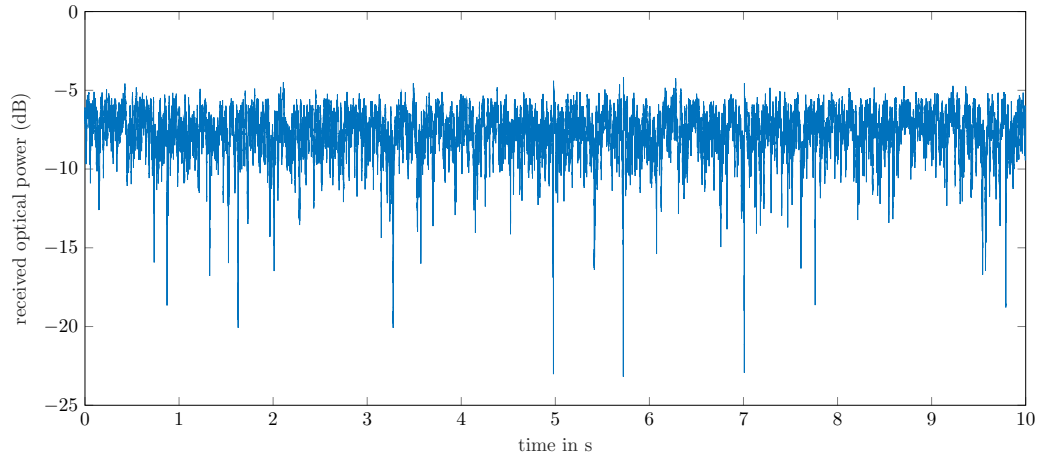


Figure 6: An example of a generated TS

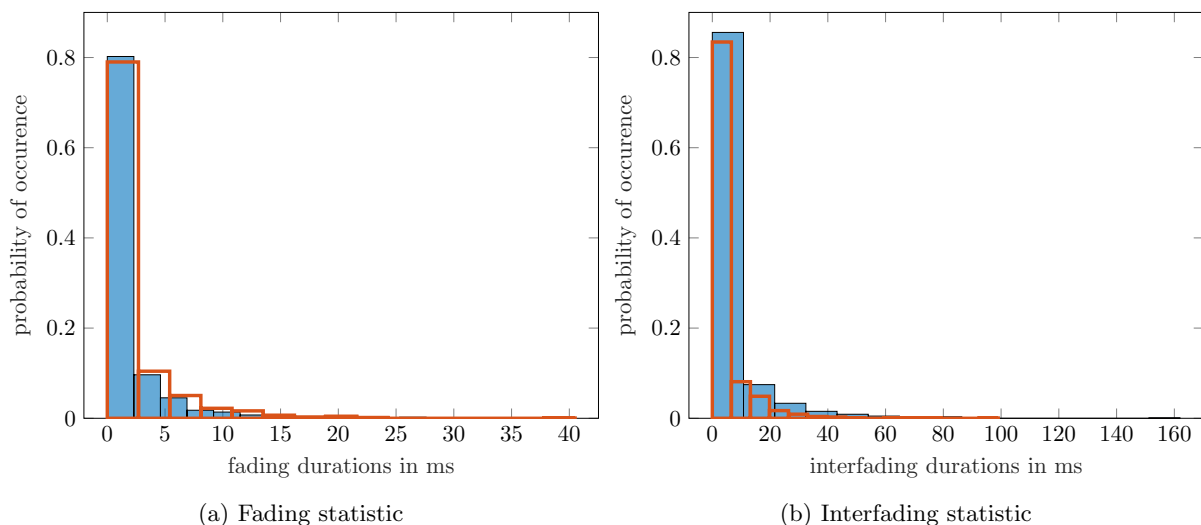


Figure 7: Fading and interfading probability of occurrence of the parent and the generated TS for a system communication threshold of  $-8\text{dB}$ . Parent TS in blue and generated TS in red

#### 4. RESULTS

Several simulations show that the above estimated log-normal distribution coupled with a MC of 50 states and a linearly spaced boundaries give satisfactory results to approximate the TS depicted in Fig. 2. Figure 6 shows a realization of a random TS generated from our proposed framework.

From a system performance point of view, we would like to compare fading statistics between the two series. Or more precisely, the fading and the inter-fading durations. As an example, suppose that we designed a communication chain that operates when the received coupled optical power is above  $-8\text{dB}$ . This thus defines (i) the fading period as the durations where the received power drops below this threshold and (ii) the interfading period where the received power is above this threshold. In Figures 7a and 7b we plot the probability mass function of different fading and interfading durations as obtained from the parent (blue) and the generated (red) TS. As one can observe, the probability mass functions are very close and are actually shown to give same performance at the system level.

#### 5. CONCLUSIONS

In this work, a simple framework was proposed to generate on the fly FSO channel time series similar to a parent TS obtained either from specialized simulation tools or real FSO transmissions. An approach combining

a distribution fitting and a Markov chain state machine was proposed. First, the distribution fitting and the optimisation of the MC parameters (number of states and the transition matrix) is performed using the parent TS. Then, once calibrated, the proposed model can be used to generate new samples according to the current state of the channel and the overall distribution. A comparison between the parent and the generated TS were compared in terms of average fading and inter-fading durations. Future work will consider other comparison criteria such as higher order moments or other types of statistical/temporal distances/divergences. Further improvements can be investigated to generalize our proposed framework to various FSO channel models such as considering higher order Markov chains.

### Acknowledgments

The authors would like to express their gratitude to Centre National d'Etudes Spatiales (CNES) for supporting this work.

### REFERENCES

- [1] Gayraud, J.-D., Maho, A., and Sotom, M., "Free-space optical communication technologies will enable next generation of ultra high throughput satellite," in [*International Conference on Space Optics—ICSO 2020*], **11852**, 2416–2424, SPIE (2021).
- [2] Roy, B., Poulenard, S., Dimitrov, S., Barrios, R., Giggenbach, D., Le Kerneç, A., and Sotom, M., "Optical feeder links for high throughput satellites," in [*2015 IEEE International Conference on Space Optical Systems and Applications (ICSOS)*], 1–6, IEEE (2015).
- [3] Mengali, A., Kourogiorgas, C. I., Lyras, N. K., Shankar Mysore Rama Rao, B., Kayhan, F., Panagopoulos, A. D., Bäumer, T., and Liolis, K., "Ground-to-geo optical feeder links for very high throughput satellite networks: Accent on diversity techniques," *International Journal of Satellite Communications and Networking* (2020).
- [4] Védrenne, N., Conan, J., Velluet, M., Sechaud, M., Toyoshima, M., Takenaka, H., Guérin, A., and Lacoste, F., "Turbulence effects on bi-directional ground-to-satellite laser communication systems," in [*International Conference on Space Optical Systems and Applications (ICSOS)*], **12** (2012).
- [5] Puryear, A., Jin, R., Lee, E., and Chan, V. W., "Experimental analysis of the time dynamics of coherent communication through turbulence: Markovianity and channel prediction," 28–37 (2011).
- [6] Lee, E. J. and Chan, V. W., "Part 1: Optical communication over the clear turbulent atmospheric channel using diversity," *IEEE journal on selected areas in communications* **22**(9), 1896–1906 (2004).
- [7] Andrews, L. C., Phillips, R. L., and Hopen, C. Y., [*Laser beam scintillation with applications*], vol. 99, SPIE press (2001).
- [8] Chen, C.-C., "Uplink channel coding for ground-to-space optical links (conference presentation)," in [*Free-Space Laser Communications XXXI*], **10910**, 109101A, SPIE (2019).
- [9] Kiasaleh, K., "Performance of apd-based, ppm free-space optical communication systems in atmospheric turbulence," *IEEE transactions on communications* **53**(9), 1455–1461 (2005).
- [10] Kiasaleh, K., "Performance of coherent dpsk free-space optical communication systems in k-distributed turbulence," *IEEE transactions on communications* **54**(4), 604–607 (2006).
- [11] Gappmair, W. and Muhammad, S. S., "Error performance of ppm/poisson channels in turbulent atmosphere with gamma-gamma distribution," *Electronics Letters* **43**(16), 880–882 (2007).
- [12] Canuet, L., Védrenne, N., Conan, J.-M., Petit, C., Artaud, G., Rissons, A., and Lacan, J., "Statistical properties of single-mode fiber coupling of satellite-to-ground laser links partially corrected by adaptive optics," *J. Opt. Soc. Am. A* **35**, 148–162 (Jan 2018).
- [13] Mushkin, M. and Bar-David, I., "Capacity and coding for the gilbert-elliott channels," *IEEE transactions on Information Theory* **35**(6), 1277–1290 (1989).